From real materials to model lattice Hamiltonians: multi-scale modelling of strongly correlated electronic systems with information from many body wavefunctions

Hitesh J. Changlani,[1] Huihuo Zheng,[2] Kiel Williams,[3] Brian Busemeyer,[3] and Lucas K. Wagner[3]

[1]*Department of Physics and Astronomy, Johns Hopkins University, Baltimore, Maryland 21218, USA*

[2]*Argonne Leadership Computing Facility, Argonne National Laboratory, 9700 South Cass Avenue, Lemont, 60439, Illinois, USA*

[3]*Department of Physics and Institute for Condensed Matter Theory, University of Illinois at Urbana-Champaign, 1110 West Green St, Urbana IL 61801, USA*

(Dated: October 1, 2017)

Given a realistic material with all its intrinsic complications, how does one develop a simple reliable model for understanding its properties? Theoretical insight has been the key driver of this process leading to simple few-band pictures. When the interactions are comparable to or much stronger than the kinetic energy, it is convenient to adopt the real space lattice approach and work with Hubbard or Kanamori type Hamiltonians involving only the low energy electrons. But this is no easy task, since the effective Hamiltonian involves a considerable renormalization of parameters with respect to the bare Coulomb values. While the kinetic energy is dominated by contributions from bands or states energetically near the Fermi level, screened interactions depend on states even *far* away from it, leading to Hubbard U's that have been traditionally hard to reliably determine. Here we discuss an approach that treats the kinetic and potential parts of the Hamiltonian democratically and one that provides a transparent way of obtaining effective Hamiltonians using data from many body wavefunctions, and whose validity can be systematically checked. We emphasize that determining the effective Hamiltonian reliably is crucial for several applications in physics and chemistry not only for quantitative accuracy, but also a correct qualitative picture of strongly correlated materials.

I. INTRODUCTION TO DOWNFOLDING THE MANY ELECTRON PROBLEM

One of the most sought-after, yet often daunting, endeavors for physicists is to develop an intuitive understanding of physical phenomena involving intrinsically complicated materials using simplified models. These models are expected to capture the essence of the physics, and are formulated in terms of the most relevant physical degrees of freedom related to the observed phenomena. For example, at high temperature and low density when quantum effects are relatively insignificant, the ideal gas model successfully captures the statistical properties of 10^{23} H_2 molecules in a box, without any detailed knowledge of the fundamental constituent of H_2. This approach is valid when we are interested in phenomena at certain energy scale (or length scale), while the degrees of freedom at other length scales which are not dynamically excited simply renormalize the dynamics of the low energy degrees of freedom.

This principle, the basis of the renormalization group [1], has also been widely employed in condensed matter physics. In the past few decades, several studies have been dedicated to describing complex systems (for example, the high T_c cuprates and other transition metal oxides), those of primary interest here are strongly correlated systems. These are systems where the effects of Coulomb interactions are comparable to or more important than the kinetic energy and the picture of localized rather than itinerant electrons is more pertinent. This has motivated an approach beyond the traditional band theory approach, involving model Hamiltonians such as the Hubbard [2], t-J [3] and Heisenberg models, defined only in terms of the valence electrons. While these models have been extensively studied analytically and numerically, and have significantly enhanced our understanding of strongly correlated physics, their effectiveness for describing a real complex system of interest is often unclear. In addition, efforts to obtain the optimal parameter values still remains very much an active area of research, often requiring experimental inputs. This is compounded by the fact that all the parameters are not independent of each other and the value of one heavily influences the value of the other. The presence of multiple competing energy scales of similar strength is, in fact, the source of rich phase diagrams that emerge under a variety of conditions - doping, pressure, temperature, all heavily dependent on material-specific properties. This motivates the need to determine reliable low energy effective Hamiltonians that can capture all the necessary details, while remaining simple enough to be simulated accurately.

The endeavor we pursue here is to develop a multi-scale approach in which the effective interactions between quasiparticles (such as dressed electrons) are determined after a *ab-initio* simula-

tion (but not necessarily exact solution) of the continuum Schroedinger equation involving all the electrons. This reduction of the Hilbert space is known as “downfolding". The resultant "lattice model" can be efficiently and accurately solved for large system sizes using techniques designed and suited for small local Hilbert spaces- these include exact or selected diagonalization [**? ?**], density matrix renormalization group (DMRG) [4], tensor networks [5–7], dynamical field theory (DMFT) [], density matrix embedding (DMET) [8] and lattice quantum Monte Carlo (QMC) methods [9**? ? ?** –14]. These methods have also been used to obtain excited states and dynamical correlation functions, that have been difficult in *ab-initio* approaches. Full *ab-initio* wavefunction based calculations are computationally infeasible for large system sizes. In addition they are often *not* accurate enough to yield an unbiased quantitative resolution of low energy scales, but *are* accurate enough to yield the correct low energy basin in which the effective description of the problem lives. This is schematically represented in Fig. **??**.

Downfolding has most commonly been carried out using approaches based on density functional theory (DFT). The kinetic part is obtained from a standard DFT calculation which is projected onto localized Wannier functions and gives an estimate of the effective hoppings of the lattice model [15]. Then, to estimate the interactions, one assumes a model of screening of the Coulomb interactions (based on RPA, for example) which is determined from the knowledge of the single particle (Kohn Sham) DFT orbitals. Since effects of interactions between the orbitals (one body space) of interest, have already been accounted for by DFT, a "double counting correction" is required to obtain the final downfolded Hamiltonian. The approach has been developed and widely applied []; a clear shortcoming is the absence of a systematic way of checking the internal accuracy of the approximation. Improving double counting estimates remains an active area of research [16].

There are other downfolding approaches that include the traditional Lowdin method, coupled to a stochastic approach [17, 18] and the related method of canonical transformations [19, 20]. These share the same aims as us, in the sense that they work with in a many body setting and involve working with wavefunctions.

Our primary focus is to downfold based on results of *ab initio* wavefunctions, involving all electrons, these explicitly provide access to properties encoded compactly in the form of reduced density matrices (RDMs) or correlation functions. Crucially, we do not commit ourselves to knowledge of exact eigenstates (a challenging endeavor) - rather we "learn" the effective Hamiltonian from a intelligently constructed database of low energy wavefunctions and their associated expec-

tation values. Our aim is thus to discuss the development and application of a new set of methods, christened "ab-initio density matrix downfolding" (AIDMD) [21],which by nature of their formulation, restore the democracy between kinetic and potential part of the Hamiltonian. There is no double counting involved and it is straightforward to judge the accuracy of the effective Hamiltonian. While our prescription applies to any wavefunction based method, we have primarily chosen to work with the *ab-initio* QMC approach [22, 23]. The QMC method works directly in the real space continuum and explicitly introduces correlations (via Jastrow factors) into trial wavefunctions of non-interacting electrons (Slater determinants). The details of the method, relevant for AIDMD, will be clarified at appropriate points in the text. More QMC related specifics are described in our earlier work [21**?**], but will not be reiterated here to focus solely on the downfolding aspect of the work.

The paper is organized as follows. In Section 2, we clarify and make precise what it means to downfold a many electron problem to a few electron problem. We recast the problem into minimization of a cost function that needs to be optimized to connect the many and few body problems. We further these notions both in terms of physical as well as information science descriptions, which allows us to connect to compression algorithms in the machine learning literature. Section 3a gives a concrete example of downfolding from the three band model (relevant to the cuprates) to the one band model - the map between the bare and effective particles and parameters will be explicitly elucidated here. These concepts are directly applied to a simple yet non-trivial *ab-initio* problem - the hydrogen chain in section 3b where we are able to systematically quantify several aspects of the effective Hubbard model describing it. Section 3c shows a more advanced application to graphene. We focus on the renormalization and screening effects that arise due to the presence of core (sigma) electrons, a comparison to its hydrogen counterpart on the honeycomb lattice clearly elucidates why graphene is a semimetal not an insulator in vacuum. Finally, in Section 4, we discuss future prospects of applications of the AIDMD method and clear avenues for methodological improvements.

II. THEORY: COMPRESSION OF THE ENERGY FUNCTIONAL/CRITERIA FOR HAMILTONIAN MATCHING

HJC: Lucas handling this section.....Look at theory.tex. Could use commented out snippets explaining Ax=E etc and criteria from theoryoldhitesh.tex

III. REPRESENTATIVE EXAMPLES

Given the theoretical framework for downfolding a many-orbital (or many electron) problem to a few orbital (or few electron) problem, we now discuss three examples which also serve to highlight some practical aspects associated with AIDMD. The first example is mostly pedagogical, where we have completely avoided the complications of low energy state generation, and the general difficulty of doing the ab-initio calculation itself. Rather, we use information directly available from *exact* eigenstates themselves to downfold from a lattice model with more orbitals (three band model) to one with fewer orbitals (one band model). We then gradually increase the complexity of the problems we address by downfolding the hydrogen chain in one dimension (with up to 10 atoms) and graphene (with up to 32 carbons on a 2D honeycomb lattice).

A. Three-band Hubbard model to one band Hubbard model at half filling

Introduction

The high T_c superconducting cuprates [24] are complex materials whose parent compounds are Mott insulators that display rich phase diagrams on electron or hole doping [25, 26]. Many extensive works have been devoted to determining their model effective Hamiltonians and corresponding parameter values [3, 15, 27–31].

The low energy physics in the cuprates is primarily associated with the 2D planes of copper and oxygen (notated as the XY plane); this setup has been shown in Fig. 1 for a 2×2 unit cell. Accounting for the octahedral environment of copper ions, with support from electronic structure and quantum chemistry calculations [25], one infers that the five-fold d orbital degeneracy of copper is lifted to make the highest singly filled orbital to be the one with $d_{x^2-y^2}$ character. The p_x or p_y oxygen orbitals (depending on their orientation relative to the copper) hybridize most strongly with $d_{x^2-y^2}$. Thus the minimal model for the cuprates involving the oxygens is the 3-orbital or 3-band Hubbard model,

$$\begin{aligned} H = \epsilon_p \sum_{j,\sigma} \epsilon_p n^p_{j,\sigma} + \epsilon_d \sum_{d} n^d_{i,\sigma} + t_{pd} \sum_{\langle i,j\rangle,\sigma} \mathrm{sgn}(p_i, d_j) \left(d^\dagger_{i,\sigma} p_{j,\sigma} + \mathrm{h.c.} \right) \\ + U_p \sum_{j} n^p_{j,\uparrow} n^p_{j,\downarrow} + U_d \sum_{i} n^d_{i,\uparrow} n^d_{i,\downarrow} + V_{pd} \sum_{\langle i,j\rangle} n^j_p n^i_d \end{aligned} \tag{1}$$

where d_i, p_j refer to the orbitals of copper (at site i) and oxygen (at site j) respectively and the

signs of the hopping t_{pd} between them are shown in Fig. 1. ϵ_p,ϵ_d refer to the orbital energies, U_d, U_p refer to strength of onsite Hubbard interactions and V_{pd} refers to the stength of the density-density interactions between a neighboring p and d orbital. One could consider further variations of the model by adding t_{pp} type hoppings, but these have not been shown here. To keep the exposition simple, we consider only the case where ϵ_p, t_{pd} and U_d are non zero and since we work with a fixed number of particles, set $\epsilon_d = 0$. Thus the charge transfer energy $\Delta \equiv \epsilon_p - \epsilon_d$ equals ϵ_p in our notation. We find it convenient to work in the hole notation and thus half filling corresponds to $2\uparrow$ and $2\downarrow$ holes on the 2×2 cell.

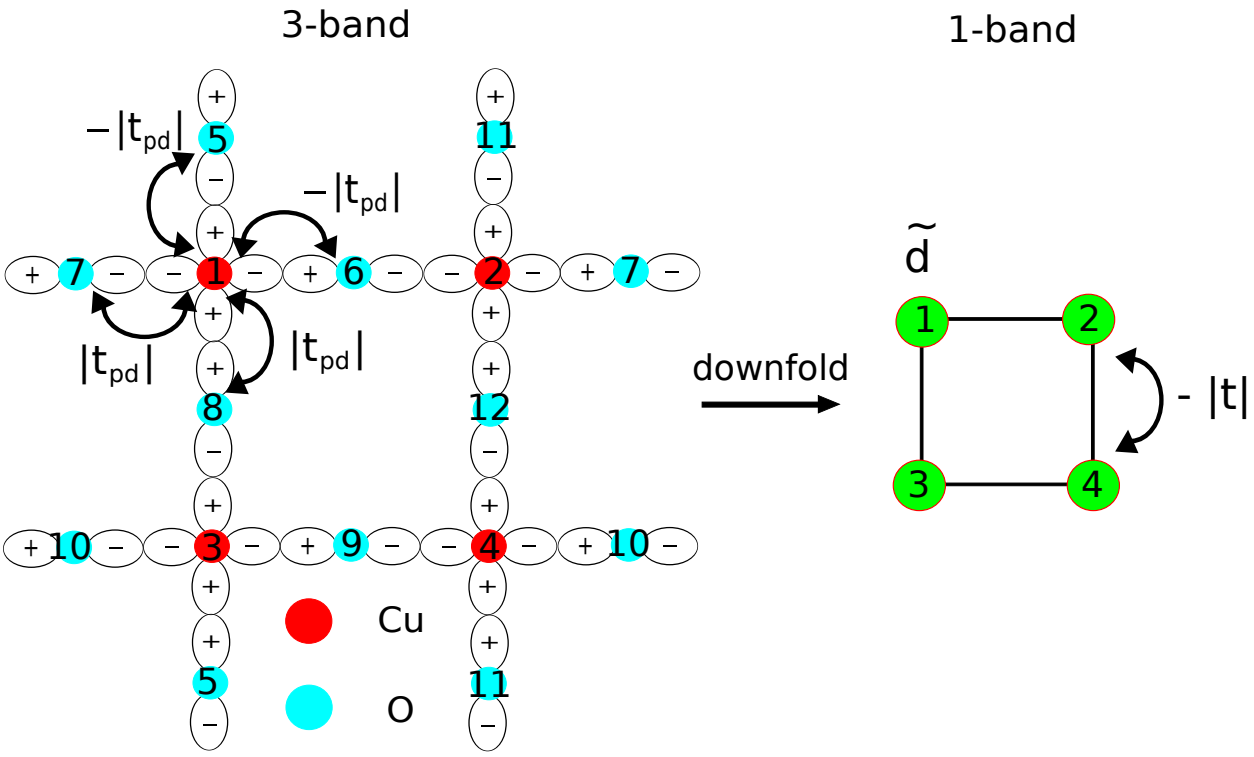

Figure 1. Schematic for downfolding the three band Hubbard model to the one band Hubbard model. The oxygen orbitals are completely eliminated to give "dressed" d-like orbitals of the one band model, with modified hopping and interaction parameters.

The justification for the 3-band model for the cuprates, along with the determination of its parameters, is itself contingent on downfolding from an *ab-initio* calculation, of the type carried out in Refs. [32]. (There is also suggestion that the 4s orbital of copper is important for the low energy properties [15] but we steer clear of these debates here.) Instead we use the 3-band model at half filling, as a prototypical example of what it *means* to downfold to a simpler model - the one

band Hubbard model,

$$\tilde{H} = -t \sum_{\langle i,j \rangle} \tilde{d}_i^\dagger \tilde{d}_j + U \sum_i \tilde{n}_\uparrow^i \tilde{n}_\downarrow^i \tag{2}$$

where t and U are downfolded (renormalized) Hubbard parameters, which are to be determined for given 3-band parameters, and $\tilde{d}$ are the effective *d-like* orbitals. The latter are a mixture of copper and oxygen orbitals and this optimal transformation also remains an unknown. Thus, the determination of effective Hamiltonians is a *dual* problem - (1) what are the composite objects that give a compact description of the low energy physics? and given this choice what are the effective interactions between them? This example will serve as a setting for the downfolding of more complex *ab-initio* systems to lattice models.

Choice of effective one particle basis

To map the three-band model to the one-band model and determine its validity, our first aim will be to obtain effective "dressed" *d-like* orbitals that enter Eq. 2. We encode this relationship as the transformation $\mathbf{T}$,

$$\tilde{d}_i = \sum_j T_{ij} c_j \tag{3}$$

where $\tilde{d}_i$ is a transformed hole (destruction) operator and c_j is the bare hole (destruction) operator, the latter could refer to either the bare d or p orbitals. Accounting for all symmetries of the 2×2 unit cell, $\mathbf{T}$ is a 4×12 matrix (the numbering of the orbitals corresponds to Fig. 1) is explicitly written out as,

$$\mathbf{T} = \begin{pmatrix} F & \alpha_2 & \alpha_2 & \alpha_4 & \alpha_1 & \alpha_1 & -\alpha_1 & -\alpha_1 & \alpha_3 & -\alpha_3 & \alpha_3 & -\alpha_3 \\ \alpha_2 & F & \alpha_4 & \alpha_2 & \alpha_3 & -\alpha_1 & \alpha_1 & -\alpha_3 & -\alpha_3 & \alpha_3 & \alpha_1 & -\alpha_1 \\ \alpha_2 & \alpha_4 & F & \alpha_2 & -\alpha_1 & \alpha_3 & -\alpha_3 & \alpha_1 & \alpha_1 & -\alpha_1 & -\alpha_3 & \alpha_3 \\ \alpha_4 & \alpha_2 & \alpha_2 & F & -\alpha_3 & -\alpha_3 & \alpha_3 & \alpha_3 & -\alpha_1 & \alpha_1 & -\alpha_1 & \alpha_1 \end{pmatrix} \tag{4}$$

where we have defined $F \equiv \sqrt{1 - 4{\alpha_1}^2 - 2{\alpha_2}^2 - 4{\alpha_3}^2 - {\alpha_4}^2}$ and where the parameters α_1,α_2,α_3 and α_4 will be optimized to minimize a certain cost function, which will be explained shortly.

Note that the transformation has been chosen to be a linear one. One can imagine a more complicated many-body transformation involving higher body functions. In practice, at least for the model under consideration, this does not seem to be necessary.

The one particle density matrix in the transformed basis is related to that in the original basis by,

$$\langle \tilde{d}_i^\dagger \tilde{d}_j \rangle = \sum_{mn} T^*_{im} \langle {c_m}^\dagger c_n \rangle T_{jn} \tag{5}$$

and using this relationship we demand two conditions be satisfied,

- ▷ The effective orbitals are orthogonal to each other
- ▷ All diagonal entries of the 1-RDM of the effective orbitals for all low energy eigenstates ($\langle \tilde{d}_i^\dagger \tilde{d}_i \rangle$) equal 1/2.

We consider a cost function,

Results and Discussion

To give a concrete and representative example of our results, we start with 1-RDM of the lowest eigenstate in either $\uparrow$ or $\downarrow$ channel. This is a 12×12 matrix, which for $U_d/t_{pd} = 8$ and $\Delta/t_{pd} = 3$ we find to be,

$$\begin{pmatrix}
+0.380 & -0.091 & -0.091 & -0.015 & +0.119 & +0.119 & -0.119 & -0.119 & -0.017 & +0.017 & -0.017 & +0.017 \\
-0.091 & +0.380 & -0.015 & -0.091 & -0.017 & -0.119 & +0.119 & +0.017 & +0.017 & -0.017 & +0.119 & -0.119 \\
-0.091 & -0.015 & +0.380 & -0.091 & -0.119 & -0.017 & +0.017 & +0.119 & +0.119 & -0.119 & +0.017 & -0.017 \\
-0.015 & -0.091 & -0.091 & +0.380 & +0.017 & +0.017 & -0.017 & -0.017 & -0.119 & +0.119 & -0.119 & +0.119 \\
+0.119 & -0.017 & -0.119 & +0.017 & +0.060 & +0.034 & -0.034 & -0.060 & -0.034 & +0.034 & -0.007 & +0.007 \\
+0.119 & -0.119 & -0.017 & +0.017 & +0.034 & +0.060 & -0.060 & -0.034 & -0.007 & +0.007 & -0.034 & +0.034 \\
-0.119 & +0.119 & +0.017 & -0.017 & -0.034 & -0.060 & +0.060 & +0.034 & +0.007 & -0.007 & +0.034 & -0.034 \\
-0.119 & +0.017 & +0.119 & -0.017 & -0.060 & -0.034 & +0.034 & +0.060 & +0.034 & -0.034 & +0.007 & -0.007 \\
-0.017 & +0.017 & +0.119 & -0.119 & -0.034 & -0.007 & +0.007 & +0.034 & +0.060 & -0.060 & +0.034 & -0.034 \\
+0.017 & -0.017 & -0.119 & +0.119 & +0.034 & +0.007 & -0.007 & -0.034 & -0.060 & +0.060 & -0.034 & +0.034 \\
-0.017 & +0.119 & +0.017 & -0.119 & -0.007 & -0.034 & +0.034 & +0.007 & +0.034 & -0.034 & +0.060 & -0.060 \\
+0.017 & -0.119 & -0.017 & +0.119 & +0.007 & +0.034 & -0.034 & -0.007 & -0.034 & +0.034 & -0.060 & +0.060
\end{pmatrix} \tag{6}$$

and transform it into a 4×4 RDM (satisfying the requirements of our cost function),

$$\begin{pmatrix}
+0.499 & -0.158 & -0.158 & 0.000 \\
-0.158 & +0.499 & 0.000 & -0.158 \\
-0.158 & 0.000 & +0.499 & -0.158 \\
0.000 & -0.158 & -0.158 & +0.499
\end{pmatrix} \tag{7}$$

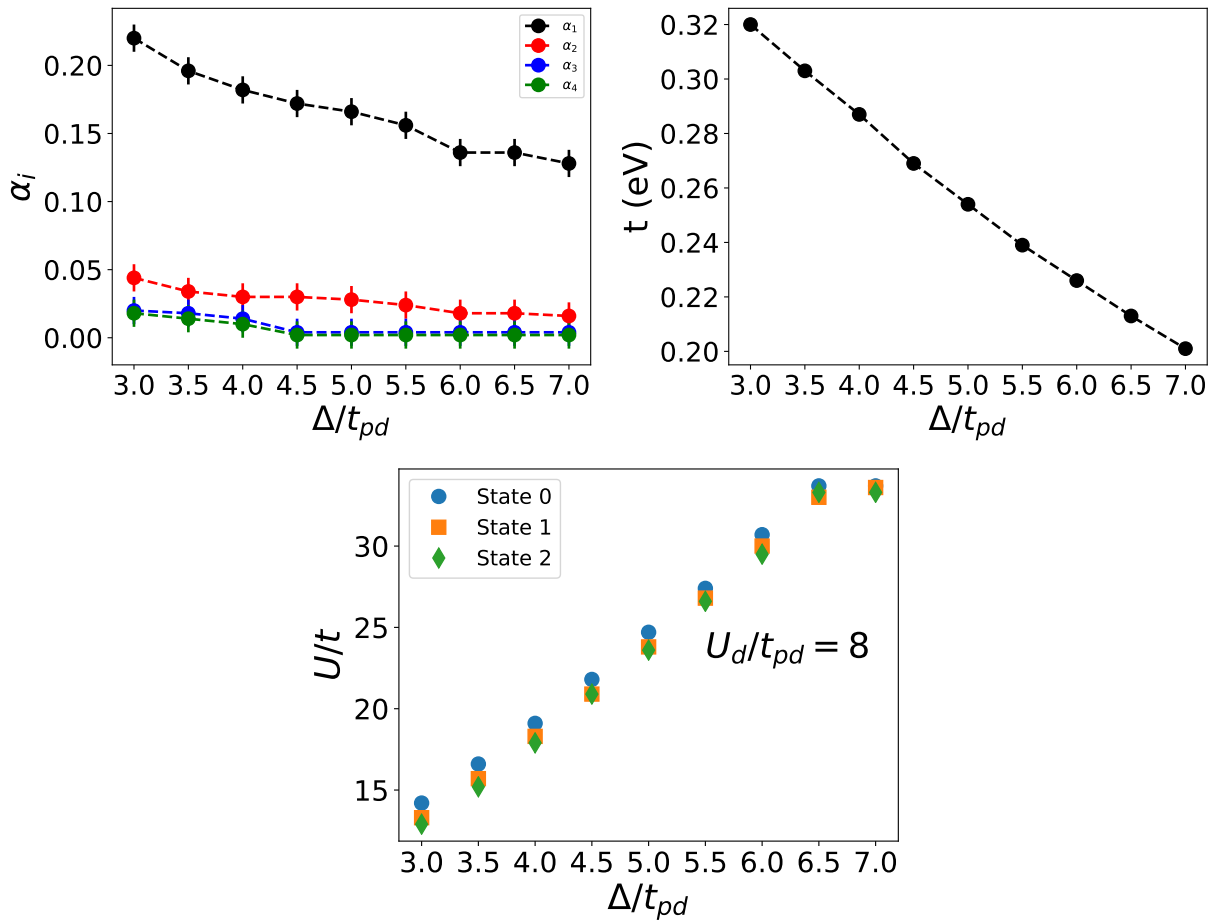

Figure 2. Downfolded values of the effective 1-band Hubbard U/t and hopping t_{opt} vs U_d/t_{pd}

corresponding to the optimal parameters $\alpha_1 = 0.220$,$\alpha_2 = 0.044$,$\alpha_3 = 0.020$ and $\alpha_4 = 0.018$ We then ask what U/t of the one band Hubbard model best describes this 1-RDM and in this case find $U/t =$. Similar results are found when one considers the other low energy eigenstates. (In practice, we minimize the sum of costs of the lowest three eigenstates on the 2×2 cluster.)

The density matrix matching does not provide an absolute energy scale for the matching. Taking t_{pd} to be the typical values of 1.3 eV, we then We show our results for the optimal values of t and the transformation parameters for different Δ/t_{pd} keeping $U_d/t_{pd} = 8$ fixed. First, note that α_1, which is the primary parameter that mixes (hybridizes) the copper and oxygen orbitals, *decreases* as Δ/t_{pd} is increased. This is physically reasonable since an increasing difference in the single particle energies of the copper and oxygen orbitals means that it is even more energetically unfavorable to occupy the oxygen orbitals. Correspondingly the effective hopping between $\tilde{d}$ in the 1-band model reduces and the effective U/t increases.

Next, we consider our results for

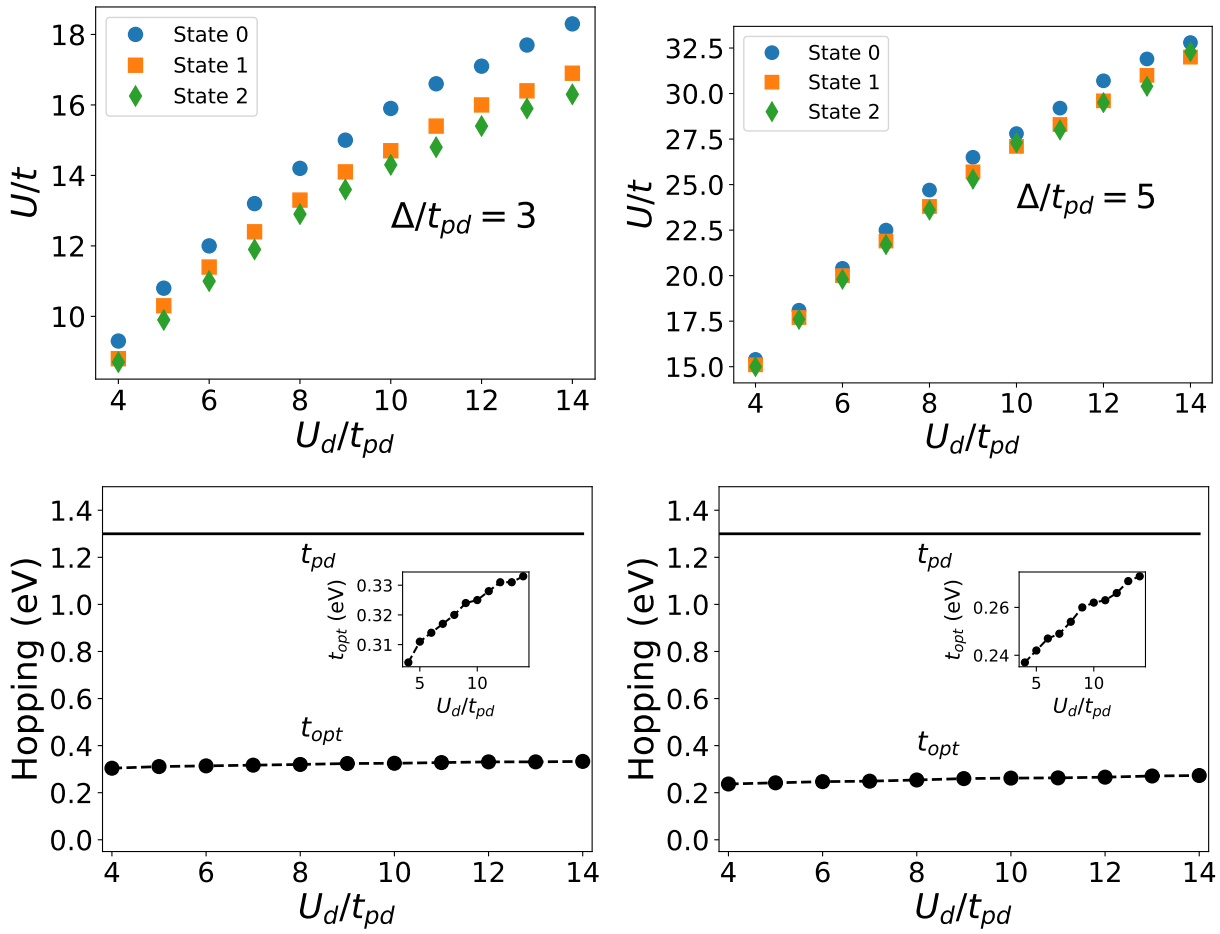

Figure 3. Downfolded values of the effective 1-band Hubbard U/t and hopping t_{opt} vs U_d/t_{pd}

These results are only useful if the energy spectra between the two models also matches. This is verified and demonstrated for some representative examples in Fig.

Finally, we show that the obtained parameters are ....

B. One dimensional hydrogen chain (Non-Eigenstate Fitting)

Let us consider the following single band model Hamiltonian,

$$H = \sum_i \left\{ -t[c^\dagger_{i\sigma} c_{i+1\sigma} + h.c.] + V n_i n_{i+1} + U n_{i\uparrow} n_{i\downarrow} + J\vec{\sigma}_i \cdot \vec{\sigma}_{i+1} \right\} + C\,. \tag{8}$$

Here, c_i's are Wannier orbitals generated from Kohn-Sham orbitals. We consider the case where the inter-atomic distance is relatively large, such that the system could be well described by a single band. We start from the 4-site hydrogen chain with bond length equals to 2Åwith periodic boundary condition. We construct the Wannier orbitals by a unitary transformation of the four low-

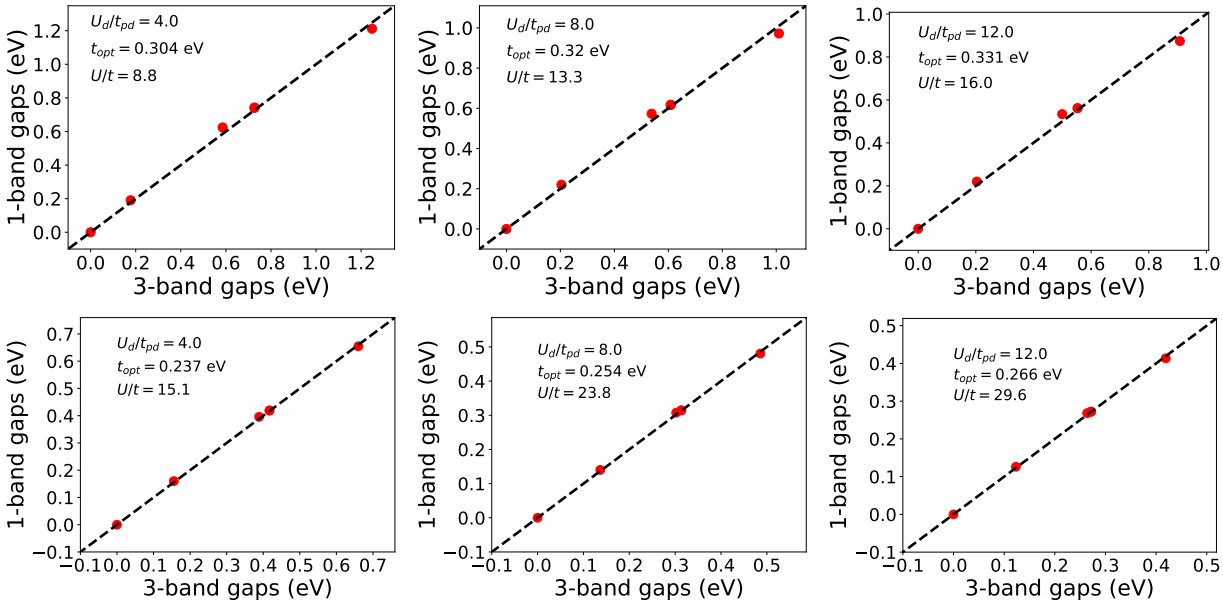

Figure 4. Comparison for energy gaps between the 3-band and 1-band Hubbard models using the optimized values of U/t and t, for different U_d/t_{pd} for $\Delta/t_{pd} = 3$ and $\Delta/t_{pd} = 5$

est energy Kohn-Sham states obtained from DFT/PBE calculation (2 occupied and 2 unoccupied). Fig. 5 shows the selected Kohn-Sham orbitals and constructed Wannier orbitals.

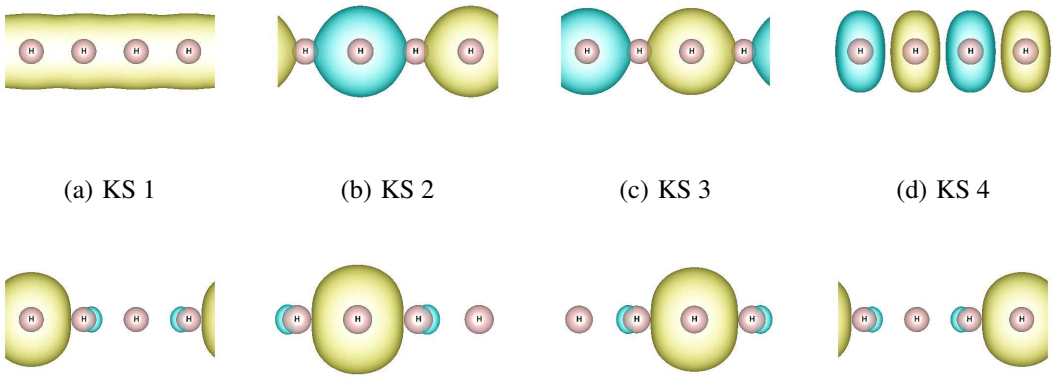

(a) KS 1 (b) KS 2 (c) KS 3 (d) KS 4

(e) Wannier 1 (f) Wannier 2 (g) Wannier 3 (h) Wannier 4

Figure 5. Kohn-Sham orbitals (upper panel) from DFT calculations with PBE exchange-exchange correlation functional, and Wannier orbitals (lower panel) constructed through a unitary transformation of Kohn-Sham orbitals.

As an alternative to the model-fitting approach for hydrogen given above, we consider fitting a model to a periodic chain of 10 hydrogen atoms, but instead using low-energy states that do not

explicitly target eigenstates of the Hamiltonian. In this example, we obtain single-particle Kohn-Sham orbitals from a set of spin-unrestricted and spin-restricted DFT-PBE calculations. With this set of orbitals, we produce a set of wave function states consisting of singles- and doubles- excitations to the Slater determinant. Allow $|S\rangle$ to be the Slater determinant formed from the Kohn-Sham orbitals, and orbitals i and j (k and l) to be Kohn-Sham orbitals that are unoccupied (occupied) in the Slater determinant. We then produce new wave function states as singles excitations $|s\rangle$ and doubles excitations $|d\rangle$ excitations to the Slater determinant:

$$|s\rangle = \quad c^\dagger_{i\sigma} c_{k\sigma} |S\rangle \tag{9a}$$

$$|d\rangle = c^\dagger_{i\sigma} c^\dagger_{j\sigma'} c_{k\sigma'} c_{l\sigma} |S\rangle, \tag{9b}$$

where σ and σ' are spin indices and $c^\dagger$ (c) is a single-electron creation (destruction) operator. This technique does not access the explicit eigenstates of the Hamiltonian, but allows many more states to be sampled in the process of characterizing the low-energy Hilbert of space of the system. The localized orbital basis upon which the descriptors are calculated is obtained by generating intrinsic atomic orbitals (IAO) from the Kohn-Sham orbitals, and localizing them using the Löwdin localization procedure.

Having produced a set of wave functions, we compute the total energies and descriptor values associated to each parameter that might appear in the model. The *ab-initio* Hamiltonian is solved using diffusion Monte Carlo (DMC) with Slater-Jastrow trial wave functions. Fig. 6 shows distributions for the U and t descriptors computed using this set of singly- and doubly-excited wave function states. Because these descriptors vary in value between the distinct states we have constructed, it is appropriate to include both within a single model.

There will exist some correlation between any two given descriptors. If two descriptors strongly covary with one another, then including both of them in a single model will introduce strong co-linearities, and produce aphysical parameter estimates. To control for this, we compute the covariance between descriptors prior to fitting a model, to verify that the descriptors are describing independent features of the wave function set. Fig. 7 shows the absolute covariance of the hopping-t descriptor with the U, J, and V descriptors as a function of the separation distance between the hydrogen ions. We see that the covariance between the t and U descriptors is consistently low across all separation distances, indicating that these parameters are describing different wave function features. Therefore these descriptors are not strongly correlated with one another, and it is appropriate to include both in a single model.

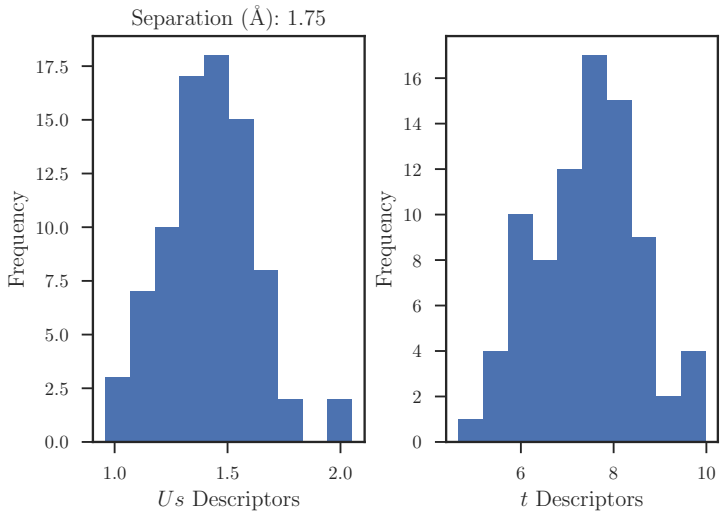

Figure 6. Histograms giving descriptor distributions for the one-body hopping t and two-body Hubbard U repulsion parameter for the periodic H_{10} chain, with a lattice constant of 1.75Å.

Having computed the energies and descriptors for this set of wave functions, and verified the independence of the U and t descriptors, we fit a Hubbard-type model to describe the *ab-initio* energetic results. Fig. 8 shows the RMS error in the resultant U-t model, relative to the *ab-initio* DMC energetics, as a function of the hydrogen inter-atomic separation. We observe the the error is consistently less than 2 eV. The fitted value of the one-body hopping t as a function of separation is shown in Fig. 9. As expected, the value of t declines toward zero at larger separations. Hence, we see that the hydrogen chain can be well-described by a Hubbard-type model for a range of inter-atomic separations.

C. Graphene and hydrogen honeycomb lattice (NE-AIDMD)

Graphene has drawn much attention in the last decade because of its unusual electronic and structural properties and its potential applications in electronics [33–40]. Although many electronic properties of graphene can be correctly described in a noninteracting electron picture [40], electron-electron interactions do play a central role in a wide range of phenomena that have been observed in experiments [41]. It is also shown that the electron screening from σ bonding is very crucial to the correlated physics of graphene, without which graphene would be an insulator instead of a semi-metal [42] .

In this section, we will use our downfolding technique to understand the electron correlations of

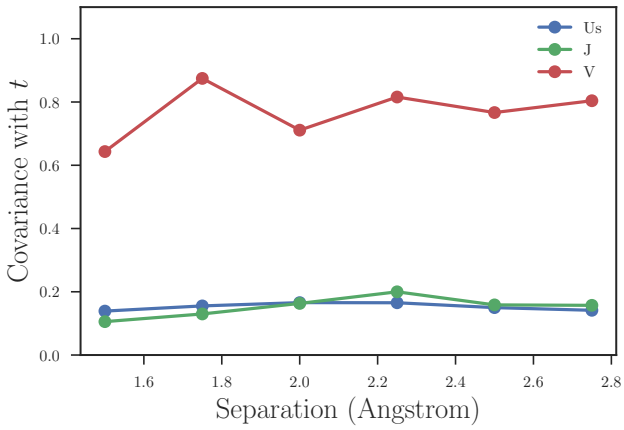

Figure 7. Covariance of the one-body hopping t descriptor with the two-body U, J, and V descriptors respectively, as a function of lattice constant for the periodic H_{10} chain. The covariance between the t and U is consistently small across all bond lengths.

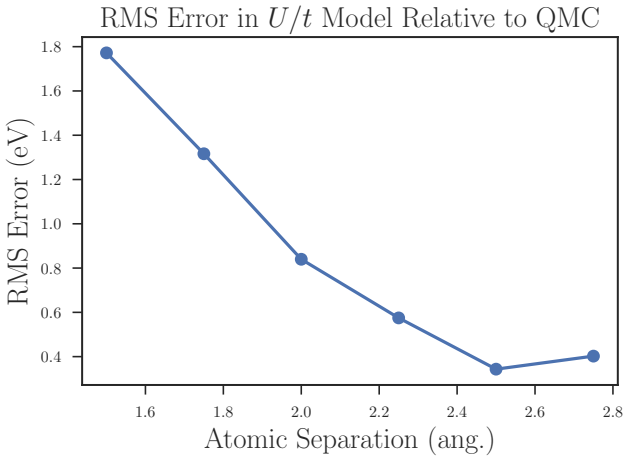

Figure 8. The RMS error in the fitted U-t model for the periodic H_{10} chain, relative to the *ab-initio* energies. The RMS error is less than 1 eV for sufficiently long bond lengths.

graphene, especially, on how the σ electrons affect the overall low energy physics. For comparison, we here also study the hydrogen honeycomb lattice with the same lattice constant $a = 2.46$Å, which has similar Dirac cone dispersion as graphene [42]. We will consider the effective single-band Hubbard model,

$$\hat{H} = C + t \sum_{\langle i,j \rangle} c^{\dagger}_{i,\sigma} c_{j,\sigma} + \text{h.c.} + U \sum_{i} n_{i,\uparrow} n_{i,\downarrow} \,. \tag{10}$$

The low energy physics is reflected mainly on the dynamics of π orbitals in graphene, and s orbitals in hydrogen. Naturally, we would choose c_i to be the π (or s) orbitals shown in Fig. 10. Due to

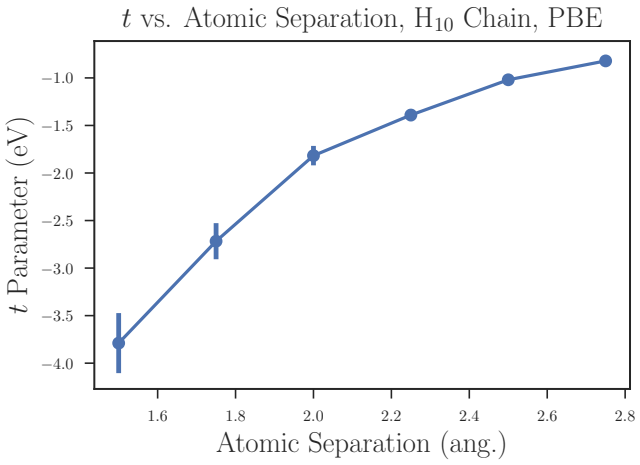

Figure 9. The one-body hopping t parameter as a function of lattice constant for the periodic H_{10} chain, obtained from a fitted U-t model. The parameter value declines to zero as the lattice constant increases.

lack of screening because of zero density of states at Fermi level, the Coulomb interaction is still long range unlike the case in metal where the Coulomb interaction is short ranged because of the formation of electron-hole pairs. However, the effect of the long range part can be considered as a renormalization to the onsite Coulomb interaction U at low energy [21, 43]. Therefore, we expect that Eq. (10) is still a relatively good description of the low energy physics.

(a) (b)

Figure 10. Wannier orbitals constructed from Kohn-Sham orbitals: (a) graphene π orbitals; (b) hydrogen S orbital.

We will use the non-eigenstate AIDMD method to obtain the value of t and U. In this way, we do not need to solve the model Hamiltonian which is relatively difficult. We choose a set of Slater-Jastrow wave functions corresponding to the electron-hole excitations within the π channel (or s channel for hydrogen system). The energy expectation expressed in terms of the density matrices is,

$$E = C + t \sum_{\langle i,j\rangle,\sigma} (\rho^{\sigma}_{ij} + \rho^{\sigma}_{ji}) + U \sum_{i} M^{\uparrow,\downarrow}_{ii;ii} \,. \tag{11}$$

In order to understand the screening effect of σ electrons, we also consider a π-only graphene, where we replace the σ electrons with constant negative charge background. The lower energy

states we choose for such systems are Slater-Jastrow wave functions constructed from occupied π Kohn-Sham orbitals; whereas for the original graphene, the wave functions are Slater-Jastrow constructed from both occupied σ bands and occupied π bands.

Table III C shows the final downfolding results of the three systems. The ab initio simulations are performed on a 3×3 cell. We have used using 25 low energy states for the downfolding. The error-bar is calculated using Jackniff method.

parameters [eV]	graphene	π-only graphene	hydrogen
t	3.61(1)	2.99	3.73(1)
U	7.16(3)	14.8(2)	9.47(5)

Table I. Downfolding parameters for graphene and hydrogen.

Fig. 11 shows fitted energies versus the *ab initio* VMC energies.

We find that the onsite Hubbard model describes graphene and hydrogen very well. The root mean square error of the predicted energies are relatively small (see Fig. 11). The ratio of U/t is small than the semi-metal-insulator transition critical value (3.8) in both graphene and hydrogen, which is consistent to the fact that both the two systems are semi-metals. The π-only graphene however has larger U/t, and is in the insulating phase. This clearly shows the significance of σ electrons in renormalizing the effective onsite interactions of π orbitals. Without such screening effect, graphene will be an insulator. This is why many previous studies incorrectly predicted graphene to be an insulator in vacuum because they consider only π electrons with bare Coulomb interaction [44–46].

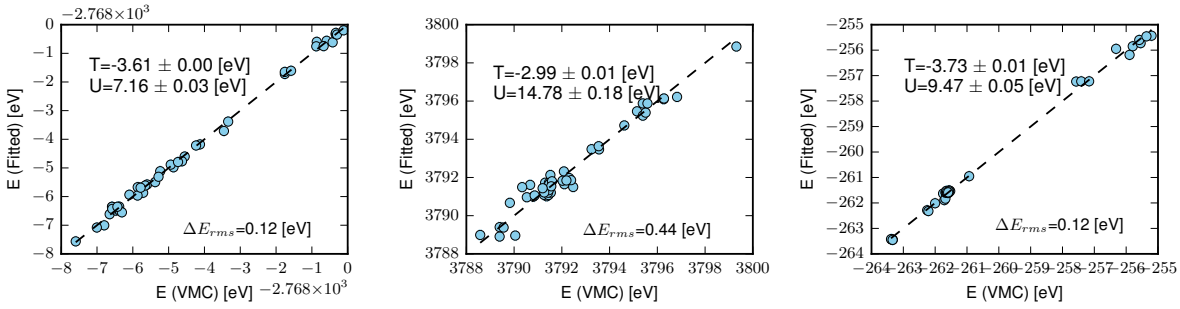

Figure 11. Comparison of *ab initio* (x-axis) and fitted energies (y-axis) of the 3×3 periodic unit cell of graphene and hydrogen lattice: (a) graphene; (b) hydrogen lattice.

IV. CONCLUSION AND FUTURE PROSPECTS

To summarize, we have explained the AIDMD method that we have been developing, primarily in conjunction with the *ab-initio* QMC approach. The practical motivation is to take data from first principles (continuum) calculations as inputs for lattice model (discrete) methods. Since one is mapping a many body problem to a few body one, the relevant quantities of interest are the reduced density matrices associated with the many-body wavefunctions projected to a one-body space. The density matrix based approach is appealing as it is democratic in the determination of the hopping and interaction parts of the effective Hamiltonian, and provides multiple checks on its validity. We have discussed three representative examples to discuss the conceptual and algorithmic aspects of AIDMD.

What sort of accuracy should one expect with effective Hamiltonians and AIDMD? The holy grail of quantum chemistry and electronic structure is to obtain an energy of 1 mHa (0.027 eV) per atom; this remains an open challenge despite decades of work. The effective Hamiltonian approach largely ameliorates this problem, only relative energies are important, neither the total energy (nor its accuracy) is of particularly fundamental interest. This, of course, is contingent on the cancellation of the large energy associated with the core electrons, whose role is to primarily renormalize the interactions between the active (valence) electrons. This aspect can also be a major limitation when the core and active electrons are strongly entangled i.e when the separation of energy scales is not prominent (in which case an energy-dependent description may be needed). Thus, it is possibly best suited for extended systems (solids) where this separation exists. In our view, AIDMD (and downfolding in general) opens up many avenues for determination of physical quantities not easily calculated in ground state approaches. Our experience suggests excitation spectra can be accurately determined to 0.2 eV (or less) [21] and potentially improved with more *ab-initio* data and more refined effective Hamiltonians.

Finally we would like to emphasize that AIDMD, though conceptually simple, is still a method in its development stages, with room for algorithmic improvements and new applications. It suffers from the usual problems of optimization and overfitting, but with advances in these fields we believe some of these major concerns may become less problematic. Some of the issues that need further research are,

- ▷ Construction of wavefunction database: The AIDMD method relies crucially on the availability of a low energy space of *ab initio* wavefunctions, which despite not being eigenstates,

reveal the nature of the effective Hamiltonian. Automating its construction remains somewhat challenging. We propose Slater Jastrow wavefunctions and deforming the orbitals entering the Slater determinant as one way of probing the low energy manifold.

▷ Optimal choice of active orbitals (one body space): In the present work, we chose DFT orbitals (in a certain energy window) and localized them to get the one body orbitals. The choice could only be justified based on looking at the trace of the 1-RDM and ensuring that it equalled the expected number of electrons. We expect to use intrinisic atomic orbitals (pointed out to us by G. K. Chan) which mitigate this issue.

▷ Form of the low energy model Hamiltonian: Extensive work in the literature has been devoted to parameterizing compact effective Hamiltonians [47–49]. Since the low energy effective Hamiltonian is not unique, there is not necessarily one right way of downfolding. One could catalogue all functional forms based on previous parameterizations or there may be some merit in determining the minimal description with fewest non zero parameters. Note that most models for strong correlation *assume* two body forms. While this appears to work well in practice, it is by not guaranteed on mathematical grounds. (Even though the Coulomb operator is two body, its low energy description need not be.)

▷ Other (non QMC) wavefunction based electronic structure methods: There are several wavefunction based quantum chemistry methods for electronic structure like coupled cluster and ab-initio DMRG which work primarily directly in orbital space. These could also be potentially explored in conjunction with AIDMD.

In terms of applications, we hope the method will be eventually applied to solids involving transition metals and/or rare earth elements, which are in the strongly correlated regime due to the presence of localized orbitals. Some challenging areas include,

▷ Spin models for magnetism: The magnetism associated with strongly correlated Mott insulators, compounded by effects such as geometrical frustration, is highly non trivial and has become an active area of research in its own right. For example, the two dimensional kagome lattice planes in herbertsmithite harbor an exotic topological phase of matter - a "quantum spin liquid". While our understanding is primarily from Heisenberg models [50, 51], contentious issues plague a complete understanding and connection to experiment (there has been recent progress in downfolding herbertsmithite [52]). Other areas of

application include pyrochlore iridates and titanates and Kitaev materials. We caution that relevant energy scales associated with magnetism can be 0.1 meV or less, and no electronic structure method is currently that accurate. It may thus be necessary to perform multiple downfolding steps to map from the Schrodinger equation to a spin model.

▷ Multiband models for superconductors: As previously mentioned, unconventional (non BCS) superconductivity in materials such as the cuprates and iron based pntictides has fuelled the study of strongly correlated systems. Several parameter sets exist in the literature for multi-band models, but it appears that there is little universal consensus. We are optimistic that additional *ab-initio* inputs from AIDMD will help constrain the part of parameter space relevant for these materials. Trends of the parameters (and the effectiveness of the three band or one band model itself) with pressure dependence and doping remain largely unexplored.

---

[1] Kenneth G. Wilson. The renormalization group: Critical phenomena and the kondo problem. *Reviews of Modern Physics*, 47(4):773–840, October 1975.

[2] J. Hubbard, Proc. R. Soc. Lond. A November 26, 1963 276 1365 238-257.

[3] K A Chao, J Spalek, and A M Oles. Kinetic exchange interaction in a narrow s-band. *Journal of Physics C: Solid State Physics*, 10(10):L271, 1977.

[4] Steven R. White. Density matrix formulation for quantum renormalization groups. *Physical Review Letters*, 69(19):2863–2866, November 1992.

[5] F. Verstraete, J. I. Cirac, arXiv:cond-mat/0407066.

[6] Hitesh J. Changlani, Jesse M. Kinder, C. J. Umrigar, and Garnet Kin-Lic Chan. Approximating strongly correlated wave functions with correlator product states. *Phys. Rev. B*, 80:245116, Dec 2009.

[7] Eric Neuscamman, Hitesh Changlani, Jesse Kinder, and Garnet Kin-Lic Chan. Nonstochastic algorithms for jastrow-slater and correlator product state wave functions. *Phys. Rev. B*, 84:205132, Nov 2011.

[8] Gerald Knizia and Garnet Kin-Lic Chan. Density matrix embedding: A simple alternative to dynamical mean-field theory. *Phys. Rev. Lett.*, 109:186404, Nov 2012.

[9] Olav F. Syljuåsen and Anders W. Sandvik. Quantum monte carlo with directed loops. *Phys. Rev. E*,

66:046701, Oct 2002.

[10] Yuan Huang, Kun Chen, Youjin Deng, Nikolay Prokof'ev, and Boris Svistunov. Spin-ice state of the quantum heisenberg antiferromagnet on the pyrochlore lattice. *Phys. Rev. Lett.*, 116:177203, Apr 2016.

[11] George H. Booth, Alex J. W. Thom, and Ali Alavi. Fermion Monte Carlo without fixed nodes: A game of life, death, and annihilation in Slater determinant space. *The Journal of Chemical Physics*, 131(5):054106, August 2009.

[12] F. R. Petruzielo, A. A. Holmes, Hitesh J. Changlani, M. P. Nightingale, and C. J. Umrigar. Semistochastic projector monte carlo method. *Phys. Rev. Lett.*, 109:230201, Dec 2012.

[13] Adam A. Holmes, Hitesh J. Changlani, and C. J. Umrigar. Efficient heat-bath sampling in fock space. *Journal of Chemical Theory and Computation*, 12(4):1561–1571, 2016. PMID: 26959242.

[14] George H. Booth, Andreas Grüneis, Georg Kresse, and Ali Alavi. Towards an exact description of electronic wavefunctions in real solids. *Nature*, 493(7432):365–370, January 2013.

[15] E. Pavarini, I. Dasgupta, T. Saha-Dasgupta, O. Jepsen, and O. K. Andersen. Band-structure trend in hole-doped cuprates and correlation with t_{cmax}. *Phys. Rev. Lett.*, 87:047003, Jul 2001.

[16] Kristjan Haule. Exact double counting in combining the dynamical mean field theory and the density functional theory. *Phys. Rev. Lett.*, 115:196403, Nov 2015.

[17] Seiichiro Ten-no. Stochastic determination of effective hamiltonian for the full configuration interaction solution of quasi-degenerate electronic states. *The Journal of Chemical Physics*, 138(16):–, 2013.

[18] S. Q. Zhou and D. M. Ceperley. Construction of localized wave functions for a disordered optical lattice and analysis of the resulting hubbard model parameters. *Phys. Rev. A*, 81:013402, Jan 2010.

[19] Steven R. White. Numerical canonical transformation approach to quantum many-body problems. *The Journal of Chemical Physics*, 117(16):7472–7482, 2002.

[20] Takeshi Yanai and Garnet Kin-Lic Chan. Canonical transformation theory for multireference problems. *The Journal of Chemical Physics*, 124(19):–, 2006.

[21] Hitesh J. Changlani, Huihuo Zheng, and Lucas K. Wagner. Density-matrix based determination of low-energy model Hamiltonians from ab initio wavefunctions. *The Journal of Chemical Physics*, 143(10):102814, September 2015.

[22] D. M. Ceperley and B. J. Alder. Ground state of the electron gas by a stochastic method. *Phys. Rev. Lett.*, 45:566–569, Aug 1980.

[23] W. M. C. Foulkes, L. Mitas, R. J. Needs, and G. Rajagopal. Quantum monte carlo simulations of solids. *Rev. Mod. Phys.*, 73:33–83, Jan 2001.

[24] J. G. Bednorz and K. A. Müller. Possible highT c superconductivity in the ba-la-cu-o system. *Zeitschrift für Physik B Condensed Matter*, 64(2):189–193, June 1986.

[25] Elbio Dagotto. Correlated electrons in high-temperature superconductors. *Rev. Mod. Phys.*, 66:763–840, Jul 1994.

[26] Patrick A. Lee, Naoto Nagaosa, and Xiao-Gang Wen. Doping a mott insulator: Physics of high-temperature superconductivity. *Rev. Mod. Phys.*, 78:17–85, Jan 2006.

[27] V. J. Emery. Theory of high-$\mathrm{t_c}$ superconductivity in oxides. *Phys. Rev. Lett.*, 58:2794–2797, Jun 1987.

[28] F. C. Zhang and T. M. Rice. Effective hamiltonian for the superconducting cu oxides. *Phys. Rev. B*, 37:3759–3761, Mar 1988.

[29] Mark S. Hybertsen, Michael Schlüter, and Niels E. Christensen. Calculation of coulomb-interaction parameters for $\mathrm{la_2cuo_4}$ using a constrained-density-functional approach. *Phys. Rev. B*, 39:9028–9041, May 1989.

[30] Mark S. Hybertsen, E. B. Stechel, M. Schluter, and D. R. Jennison. Renormalization from density-functional theory to strong-coupling models for electronic states in cu-o materials. *Phys. Rev. B*, 41:11068–11072, Jun 1990.

[31] P. R. C. Kent, T. Saha-Dasgupta, O. Jepsen, O. K. Andersen, A. Macridin, T. A. Maier, M. Jarrell, and T. C. Schulthess. Combined density functional and dynamical cluster quantum monte carlo calculations of the three-band hubbard model for hole-doped cuprate superconductors. *Phys. Rev. B*, 78:035132, Jul 2008.

[32] Lucas K. Wagner and Peter Abbamonte. Effect of electron correlation on the electronic structure and spin-lattice coupling of high-T_c cuprates: Quantum monte carlo calculations. *Phys. Rev. B*, 90:125129, Sep 2014.

[33] P. R. Wallace. The band theory of graphite. *Physical Review*, 71(9):622, May 1947.

[34] K. S. Novoselov, A. K. Geim, S. V. Morozov, D. Jiang, Y. Zhang, S. V. Dubonos, I. V. Grigorieva, and A. A. Firsov. Electric Field Effect in Atomically Thin Carbon Films. *Science*, 306(5696):666–669, October 2004.

[35] K. S. Novoselov, A. K. Geim, S. V. Morozov, D. Jiang, M. I. Katsnelson, I. V. Grigorieva, S. V. Dubonos, and A. A. Firsov. Two-dimensional gas of massless dirac fermions in graphene. *Nature*, 438(7065):197–200, 2005.

[36] M. I. Katsnelson, K. S. Novoselov, and A. K. Geim. Chiral tunnelling and the klein paradox in graphene. *Nat Phys*, 2(9):620–625, 2006.

[37] A. K. Geim and K. S. Novoselov. The rise of graphene. *Nature Materials*, 6(3):183–191, 2007.

[38] K. S. Novoselov, Z. Jiang, Y. Zhang, S. V. Morozov, H. L. Stormer, U. Zeitler, J. C. Maan, G. S. Boebinger, P. Kim, and A. K. Geim. Room-temperature quantum hall effect in graphene. *science*, 315(5817):1379–1379, 2007.

[39] A. H. Castro Neto, F. Guinea, N. M. R. Peres, K. S. Novoselov, and A. K. Geim. The electronic properties of graphene. *Reviews of Modern Physics*, 81(1):109, January 2009.

[40] A. H. Castro Neto, F. Guinea, N. M. R. Peres, K. S. Novoselov, and A. K. Geim. The electronic properties of graphene. *Reviews of Modern Physics*, 81(1):109, January 2009.

[41] Valeri N. Kotov, Bruno Uchoa, Vitor M. Pereira, F. Guinea, and A. H. Castro Neto. Electron-Electron Interactions in Graphene: Current Status and Perspectives. *Reviews of Modern Physics*, 84(3):1067–1125, July 2012.

[42] Huihuo Zheng, Yu Gan, Peter Abbamonte, and Lucas K. Wagner. The importance of sigma bonding electrons for the accurate description of electron correlation in graphene. *arXiv:1605.01076 [cond-mat]*, 2016.

[43] M. Schüler, M. Rösner, T. O. Wehling, A. I. Lichtenstein, and M. I. Katsnelson. Optimal Hubbard Models for Materials with Nonlocal Coulomb Interactions: Graphene, Silicene, and Benzene. *Physical Review Letters*, 111(3):036601, July 2013.

[44] JoaquÃ¯Â¿Âœn E. Drut and Timo A. Lähde. Is Graphene in Vacuum an Insulator? *Physical Review Letters*, 102(2):026802, January 2009.

[45] JoaquÃ¯Â¿Âœn E. Drut and Timo A. Lähde. Critical exponents of the semimetal-insulator transition in graphene: A Monte Carlo study. *Physical Review B*, 79(24):241405, June 2009.

[46] Dominik Smith and Lorenz von Smekal. Monte carlo simulation of the tight-binding model of graphene with partially screened coulomb interactions. *Physical Review B*, 89(19):195429, 2014.

[47] Antoine Georges, Luca de' Medici, and Jernej Mravlje. Strong correlations from hund's coupling. *Annual Review of Condensed Matter Physics*, 4(1):137–178, 2013.

[48] A. M. Oles and G. Stollhoff. Correlation effects in ferromagnetism of transition metals. *Phys. Rev. B*, 29:314–327, Jan 1984.

[49] M. E. A. Coury, S. L. Dudarev, W. M. C. Foulkes, A. P. Horsfield, Pui-Wai Ma, and J. S. Spencer. Hubbard-like hamiltonians for interacting electrons in s, p, and d orbitals. *Phys. Rev. B*, 93:075101,

Feb 2016.

[50] Simeng Yan, David A. Huse, and Steven R. White. Spin-liquid ground state of the s = 1/2 kagome heisenberg antiferromagnet. *Science*, 332(6034):1173–1176, 2011.

[51] H. J. Changlani, D. Kochkov, K. Kumar, B. K. Clark, and E. Fradkin. The mother of all states of the kagome quantum antiferromagnet. *ArXiv e-prints*, March 2017.

[52] Harald O. Jeschke, Francesc Salvat-Pujol, and Roser Valentí. First-principles determination of heisenberg hamiltonian parameters for the spin-$\frac{1}{2}$ kagome antiferromagnet $zncu_3(oh)_6cl_2$. *Phys. Rev. B*, 88:075106, Aug 2013.